Microelectronic Engineering xxx (2013) xxx–xxx

Contents lists available at SciVerse ScienceDirect

Microelectronic Engineering

journal homepage: www.elsevier.com/locate/mee

Gate capacitance modeling and width-dependent performance of graphene nanoribbon transistors

George S. Kliros *

Department of Aeronautical Sciences, Division of Electronics and Communications Engineering, Hellenic Air-Force Academy, Dekeleia Air-Force Base GR-1010, Attica, Greece

ARTICLE INFO

Article history:
Available online xxxx

Keywords:
Graphene FETs
Graphene nanoribbons
Gate capacitance
Analytic ballistic model
Performance metrics

ABSTRACT

The width-dependent performance of armchair GNRs-FETs is investigated by developing a fully analytical gate capacitance model based on effective mass approximation and semiclassical ballistic transport. The model incorporates the effects of edge bond relaxation and third nearest neighbor interaction as well as thermal broadening. To calculate the performance metrics of GNR-FETs, analytical expressions are used for the charge density, quantum capacitance as well as drain current as functions of both gate and drain voltages. Intrinsic gate delay time, cutoff frequency and I_{on}/I_{off} ratio are also calculated for different GNR widths. Numerical results for a double-gate AGNR-FET operating close to quantum capacitance limit show that nanoribbon widths of about 3–4 nm at most are required in order to obtain optimum on/off performance.

1. Introduction

Graphene, has recently emerged as a potential candidate for nanoelectronics since its high mobility and carrier velocity promises ballistic devices with high switching speeds [1–3]. In graphene, the charge carriers in the two-dimensional (2D) channel can change from electrons to holes with the application of an electrostatic gate with a minimum density at the charge neutrality point (Dirac point) characterizing the transition. However, the on-current to off-current ratio of graphene channel field effect transistors (FETs) is very small due to the lack of a bandgap. As a result, monolayer graphene is not directly suitable for digital circuits, but is very promising for analog, high frequency applications [4]. Interestingly, if graphene is patterned into nanoribbons, using planar technologies such as electron beam lithography and etching, a sizeable bandgap opens due to quantum confinement effect in the transverse direction. The bandgap of a GNR depends on its width and edge orientation. Zigzag edged nanoribbons have a very small gap due to localized edge states. No such localized state appears in an armchair graphene nanoribbon (AGNR). Using first principle approach, Son et al. [5] have shown that the band gap of an AGNR arises from both the quantum confinement and the edge effects. As a consequence, FETs with AGNR channels (AGNR-FETs), showing complete switch off and improved on–off current ratios, can be considered as building blocks for future digital circuits.

Numerical modeling of GNR-FETs is usually based on a 'top-of-the barrier' approach under ballistic transport [6,7]. An extension of this approach in order to describe both ballistic and diffusive transport in graphene devices has been recently proposed [8]. More accurate 'atomistic' models are based on self-consistent non-equilibrium Green's Function (NEGF) formalism in both real and mode space basis [9,10], in some cases including phonon scattering [11] and disorder [12]. Such atomistic numerical models are computationally very expensive and motivate the need for analytical modeling [13,14]. Zhao et al. [14,15] have proposed a semi-analytical model for the characteristics of GNR-FETs which requires an iterative procedure for calculating the top of the barrier potential, carrier concentration and quantum capacitance for each bias point. In this work, the performance of armchair GNR-FETs is investigated by developing a fully analytical ballistic model where the carrier concentration is calculated by using the effective mass approximation in the density of states along with a well known relation between gate voltage and source Fermi energy [22]. Effective mass approximation is quite accurate in narrow GNRs since their band dispersion curves are approximately parabolic. Moreover, since edge bond relaxation and third nearest neighbor (3NN) interaction have great impact on the band structure of GNRs [16], we have considered these factors in our calculations. The model is simple and computationally efficient with no iterations or numerical integration involved. In order to calculate the performance metrics of GNR-FETs, analytical expressions are provided for the charge density, quantum capacitance as well as drain current as functions of gate voltage. Gate delay time, power-delay time product and cutoff frequency are calculated for different GNR widths. Since significant performance improvement is expected for nanodevices in the quantum capacitance limit QCL [17], a double-gate AGNR-FET operating close to QCL, is considered.

* Tel.: +30 211 400 2009; fax: +30 210 8074606.
E-mail address: gskliros@ieee.org

0167-9317/$ - see front matter © 2013 Elsevier B.V. All rights reserved.
http://dx.doi.org/10.1016/j.mee.2013.04.011

2. Device structure

The device structure used in our study is shown in Fig.1(a). Double-gate geometry is considered with gate-insulator HfO_2 of thickness $t_{ins} = 1$ nm and relative dielectric constant κ=16. The source and the drain region are assumed to be highly doped extensions of the GNR channel so that the source Fermi energy entered the conduction band. The power supply is set $V_{DD} = 0.5$ V and room temperature (T = 300 K) is assumed. Since thin and high-κ gate insulator is employed, we can expect excellent gate control to prevent source-drain direct tunneling. Moreover, the quantum capacitance limit (QCL), where the small quantum capacitance dominates the total gate capacitance, can be reached. As it is known [17,24], in the QCL, the potential distribution within the channel is determined by the gate potential rather than the channel charge and thus, electrostatic short channel effects are suppressed. However, to account for such effects that may be important when the device operates far from the QCL, phenomenological capacitances describing the electrostatic coupling between the channel and the source/drain should be considered [15]. Fig. 1(b) shows the atomic structure of armchair graphene nanoribbon (AGNR) where carbon atoms are arranged in a honeycomb lattice and carbon–carbon (C–C) bonds at the edges are bonded to hydrogen atoms to terminate dangling bonds. All C–C bond lengths are taken as $a_{cc} = 0.142$ nm and hence, the width of the ribbon is given by $W = (N+1)\sqrt{3}a_{cc}/2$, where N is the number of atoms in its transverse direction [16].

3. Simulation model

3.1. Effective mass and band structure

In order to proceed with the development of an analytical model based on the effective mass approximation, we first need an expression for the energy bands of AGNRs. It has been verified that a 3NN tight binding model incorporating the edge-bond relaxation can accurately predict the band structure of GNRs [16]. The 2NN interaction, which only shifts the dispersion relation in the energy axis but does not change the band structure, can be ignored. Using a Taylor expansion around the charge neutrality point, the band structure of an AGNR can be written as [16]

$$E_n^{\pm}(k_x) = \pm\sqrt{E_{C,n}^2 + (\hbar\upsilon_n k_x)^2} \tag{1}$$

with

$$E_{C,n} = \gamma_1(1 + 2s\cos(n\theta)) + \gamma_3(1 + 2\cos(2n\theta)) + \frac{4(\gamma_3 + \Delta\gamma_1)}{N+1}\sin^2(n\theta) \tag{2}$$

and

$$(\hbar\upsilon_n)^2 = (3a_{cc})^2\left[-\frac{1}{2}s\gamma_1\cos(n\theta)\times\left(\gamma_1 + \gamma_3(1+2\cos(2n\theta) + \frac{4(\gamma_3+\Delta\gamma_1)}{N+1}\sin^2(n\theta)\right)\right.$$
$$\left.-\gamma_3\left(\gamma_1 + 2\gamma_3\cos(2n\theta) + \frac{4(\gamma_3+\Delta\gamma_1)}{N+1}\sin^2(n\theta)\right)\right] \tag{3}$$

where $\theta = \pi/(N+1)$, $\pm$ indicates the conduction band and valence band respectively, N is the total number of carbon atoms in the ribbon, n denotes the subband index, and $E_{C,n}$ is the band edge energy of the nth subband. The first set of conduction and valence bands have band index $s = -1$. Due to the symmetric band structure of electrons and holes, one obtains for the energy gap $E_{G,n} = 2E_{C,n}$. Also, $\gamma_1 = -3.2eV$ and $\gamma_3 = -0.3eV$ refer to the first and third-nearest neighbor hopping parameters and $\Delta\gamma_1 = -0.2eV$ is used for the correction to γ_1 due to edge bond relaxation effect. The electron effective masses at the bottom of the conduction band is given by

$$m_n^* = \frac{E_{C,n}}{\upsilon_n^2}. \tag{4}$$

It is worth noting that the electron effective mass is an energy-dependent variable which can be calculated using the $E-k$ dispersion relation. A plot of the effective mass of the first conduction band (in units of the free electron mass), as a function of electron energy for AGNR of different widths, is shown in Fig. 2(a). As it is seen, the effective mass is very low at the band minimum, however, as we move away from the band minimum, it increases rapidly with energy. Moreover, GNRs with $N = 3p+1$, where p is an integer, have larger effective masses at the conduction band minimum than the GNRs with $N = 3p$. An additional point for each GNR-family is that, at a given energy away from the band minimum, the increase of the GNR width causes the increase of effective mass. On the other hand, as is shown in Fig. 2(b), the effective mass at the band minimum decreases as the ribbon width increases.

Assuming a ballistic channel, the carriers with $+k$ and $-k$ states are in equilibrium with Fermi energies of the source (E_{FS}) and the drain (E_{FD}) respectively, with $E_{FS} = E_F$ and $E_{FD} = E_F - qV_D$. Thus, the carrier density inside the channel is given by

$$n_{1D} = \frac{1}{2}\int_{E_{C,n}}^{\infty} D(E)[f_S(E) + f_D(E)]dE \tag{5}$$

where

$$D(E) = \frac{1}{\pi\hbar}\sum_{n>0}\frac{\sqrt{2m_n^*}}{\sqrt{E - E_{C,n}}}\Theta(E - E_{C,n}) \tag{6}$$

is the total 1D density of states (DOS) and Θ denotes the unit step function. $f_{S,D}(E)$ are the Fermi–Dirac probabilities which, at temperature T, are expressed as

$$f_{S,D}(E) = \frac{1}{1 + e^{(E-E_{FS,D})/k_BT}} \tag{7}$$

where k_B is the Boltzmann constant. After integrating, Eq. (5) yields

$$n_{1D} = \sqrt{\frac{k_BT}{2\pi\hbar^2}}\sum_{n>0}\sqrt{m_n^*}\left[F_{-1/2}(\eta_{n,S}) + F_{-1/2}(\eta_{n,D})\right] \tag{8}$$

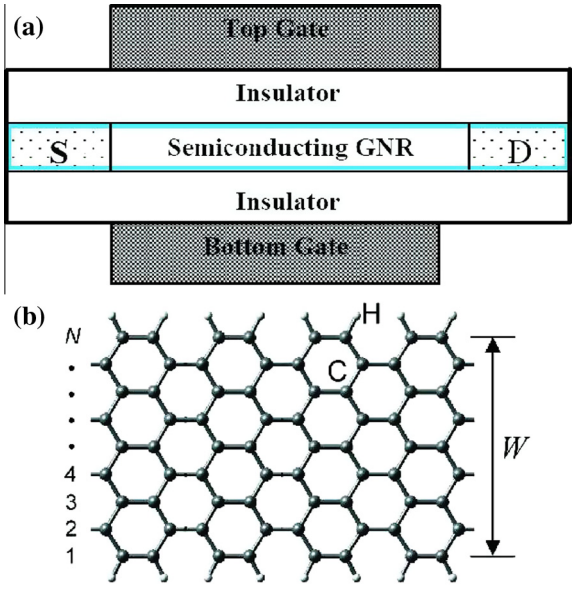

Fig. 1. (a) Schematics of double-gate GNR FET where a semiconducting AGNR is used as channel material. (b) The atomic structure of an AGNR where all edge dangling bonds are terminated by hydrogen atoms.